CRLX101, a nanoparticle-drug conjugate containing camptothecin, improves rectal cancer chemoradiotherapy by inhibiting DNA repair and HIF-1α

Xi Tian[1], **Minh Nguyen**[1], **Henry P. Foote**[1], **Joseph M. Caster**[1], **Kyle C. Roche**[1], **Christian G. Peters**[2], **Pauline Wu**[2], **Lata Jayaraman**[2], **Edward G. Garmey**[2], **Joel E. Tepper**[1], **Scott Eliasof**[2], and **Andrew Z. Wang**[1,*]

[1]Department of Radiation Oncology, Lineberger Comprehensive Cancer Center, Carolina Center for Cancer Nanotechnology Excellence, Carolina Institute of Nanomedicine, University of North Carolina at Chapel Hill, Chapel Hill, NC 27599, USA

[2]Cerulean Pharma Inc, 840 Memorial Drive, Cambridge, MA 02139

Abstract

Novel agents are needed to improve chemoradiotherapy for locally advanced rectal cancer. In this study, we assessed the ability of CRLX101, an investigational nanoparticle-drug conjugate containing the payload camptothecin (CPT), to improve therapeutic responses as compared to standard chemotherapy. CRLX101 was evaluated as a radiosensitizer in colorectal cancer cell lines and murine xenograft models. CRLX101 was as potent as CPT *in vitro* in its ability to radiosensitize cancer cells. Evaluations *in vivo* demonstrated that the addition of CRLX101 to standard chemoradiotherapy significantly increased therapeutic efficacy by inhibiting DNA repair and HIF-1α pathway activation in tumor cells. Notably, CRLX101 was more effective than oxaliplatin at enhancing the efficacy of chemoradiotherapy, with CRLX101 and 5-fluorouracil (5-FU) producing the highest therapeutic efficacy. Gastrointestinal toxicity was also significantly lower for CRLX101 compared to CPT when combined with radiotherapy. Our results offer a preclinical proof of concept for CRLX101 as a modality to improve the outcome of neoadjuvant chemoradiotherapy for rectal cancer treatment, in support of ongoing clinical evaluation of this agent (LCC1315 NCT02010567).

Introduction

It is estimated that 40,000 patients are diagnosed with rectal cancer, and that approximately 22,000 patients die from this disease in the United States each year (1). While some patients present with early disease that can be cured with surgical resection alone, many patients present with locally advanced disease (T3, and/or N+) that requires neoadjuvant chemoradiotherapy (CRT) followed by surgical resection (2). The standard neoadjuvant CRT regimen consists of administering either infusional 5-fluorouracil (5-FU) or oral

*Corresponding Author: Andrew Zhuang Wang, Department of Radiation Oncology, Lineberger Comprehensive Cancer Center, CB 7512, UNC Chapel Hill, Chapel Hill, North Carolina, 27514, (P) 919-966-7700, (F) 919-966-7681, zawang@med.unc.edu.

capecitabine with approximately 50 Gy of radiotherapy to the pelvis. In addition to neoadjuvant CRT, postoperative CRT has also proved beneficial (3). A few clinical trials have shown that rectal cancer patients receiving CRT after surgical resection demonstrate reduced rates of local recurrence and improved survival when compared to patients receiving surgery alone (4–6). For these reasons, CRT represents an important treatment strategy for rectal cancer.

A number of studies have suggested that CRT alone may be an effective rectal cancer treatment strategy. Several large randomized trials have demonstrated that 8–25% of patients receiving only CRT achieve a pathologic complete response (pCR) (7–13). Importantly, patients who achieve a pCR also achieve improved overall and recurrence free survival (14–16). Moreover, recent clinical studies have suggested that surgery can be omitted in patients with pCR to preserve organ integrity and quality of life (17). Therefore, identifying therapeutic agents that can be combined with standard CRT to improve the pCR rates of rectal cancer patients has been an active area of research (18).

Many clinical trials have evaluated whether pCR rates of CRT can be improved via the inclusion of additional therapeutic agents to 5-FU and radiotherapy. Specifically, trials have evaluated the effect of adding chemotherapeutics (oxaliplatin and irinotecan) and targeted antibodies (bevacizumab and cetuximab) to standard CRT. Clinical studies evaluating the addition of oxaliplatin (Ox) to standard CRT showed increased toxicity with no added therapeutic benefit (12,19). Although some trials have shown that the addition of irinotecan improves pCR rates in rectal cancer patients (20), the clinical adoption of this treatment strategy was prevented by unacceptable off-target toxicity (21,22). The use of targeted therapies such as bevacizumab and cetuximab with standard CRT has yielded mixed results and, therefore, has not been integrated into standard treatment regimens (9). Consequently, there remains great interest in the development of novel agents that can be combined with established CRT regimens to improve rectal cancer treatment.

Inhibitors of topoisomerase 1 (topo-1), including the marketed drugs irinotecan and topotecan, are well known radiosensitizers (23). Irinotecan is highly effective against colorectal cancer, but it produces unacceptable gastrointestinal (GI) toxicity when combined with radiotherapy (20). Camptothecin (CPT) has been shown to be an effective treatment for rectal cancer in preclinical studies, but it could not be developed clinically because it was not well tolerated. The recent clinical development of CRLX101, an investigational nanoparticle-drug conjugate containing the payload CPT, offers a unique opportunity to improve CRT for rectal cancer. CRLX101 is a nanoparticle consisting of CPT (10% by weight) conjugated to a biocompatible copolymer of cyclodextrin and polyethylene glycol (PEG) (24). CRLX101 nanoparticles have diameters ranging from 20 to 30 nm and a slightly negative ζ–potential (−5 mV) (24). Physiologically, CRLX101 has been shown to be a potent inhibitor of topo-1 and hypoxia-inducible factor-1 alpha (HIF-1α), a signaling molecule that promotes radioresistance in cancer cells (24–26). Currently, CRLX101 is being evaluated in phase II trials as both a monotherapy and in combination with other anti-cancer drugs as a treatment strategy for several tumor types (27).

CRLX101 has several attractive properties that may improve CRT. First, CRLX101, as a nanoparticle, preferentially accumulates in tumors through the enhanced permeability and retention (EPR) effect (28,29). Secondly, CRLX101 has not demonstrated any significant GI toxicity to date (27, 30). Thirdly, CRLX101 has a long circulation time (circulation half-life of 17.2 h) (31). In addition, CRLX101 releases CPT in a prolonged fashion, which is particularly conducive for radiosensitization during fractionated radiotherapy (16). Lastly, CRLX101 has the potential to promote radiosensitization through two independent mechanisms, inhibition of topo-1 and HIF-1α (25).

Given the radiosensitizing potential that CPT has demonstrated in preclinical studies, we hypothesized that the efficacy of standard CRT would be significantly improved by the addition of CRLX101. Therefore, we evaluated whether the addition of CRLX101 to 5-FU and radiotherapy could improve rectal cancer treatment using preclinical rectal cancer models. Our study supports the ongoing clinical investigation of CRLX101 in rectal cancer CRT.

Materials and Methods

Materials

CRLX101 was provided by Cerulean Pharma Inc. (Cambridge, MA). Each gram of CRLX101 contained 100 mg of CPT. CRLX101 was re-suspended in phosphate buffer saline. Camptothecin was purchased from ACROS Organics (Fair Lawn, NJ). 5-Fluorouracil (5-FU) and Oxaliplatin (Ox) were purchased from Sigma-Aldrich.

Mice

Nu/Nu mice (male, 7–8 weeks old) were obtained from the animal colony at the University of North Carolina (UNC) Lineberger Comprehensive Cancer Center (LCCC). C57BL/6J mice (male, 8 weeks old) were purchased from The Jackson Laboratory (Bar Harbor, ME). All animal experiments were performed in accordance with guidelines from the UNC Institutional Animal Care and Use Committee.

Cell Culture

Human colorectal cancer cell lines HT-29 (ATCC batch F-9246) and SW480 cells (ATCC batch 7265) were obtained from the Tissue Culture Facility at the LCCC at UNC in 2014. Cell line authentication was performed via short tandem repeat in 2014. The luciferase-expressing cell line HT-29-luc2 was purchased from Caliper Life Sciences (Hopkinton, MA) in 2014. All cell lines were used within 10 passages after initial plating. HT-29, SW480, and HT-29-luc2 cells were cultured at 37°C in 5% CO_2 humidified atmosphere in Dulbecco's Modified Eagle Medium: Nutrient Mixture F-12 (DMEM/F12) (Gibco) supplemented with 10% (vol/vol) fetal bovine serum (Gibco) and 1% penicillin/streptomycin (Gibco).

X-Ray Irradiation

Cells and mice were irradiated using a Precision X-RAD 320 (Precision X-Ray, Inc) machine operating at 320 kVp and 12.5 mA. For tumor growth assays, a 3 mm lead shield protected the mice's vital organs, and the left flank remained exposed during irradiation. In

order to test hair loss toxicity, a 0.5 cm thick bolus covered the left dorsal region of the mice during irradiation to enhance the skin dose. For GI toxicity, the entire pelvic region was irradiated while a 3mm lead shield protected the legs, upper abdomen, thoracic region, and head of the mouse.

Cell Viability Assay

Cells were seeded at 10,000 cells/well in 96-well plates. Cells were treated with CRLX101, CPT, or PBS (control) for 24 hours, washed with PBS after incubation, and incubated in fresh, complete medium for 24 hours. Following incubation, MTS [(3-(4,5-dimethylthiazol-2-yl)-5-(3-car- boxymethoxyphenyl)-2-(4-sulfophenyl)-2H-tetrazolium)] cell proliferation assays were performed according to manufacturer protocols using the CellTiter 96® Aqueous One Solution Cell Proliferation assay kit (Promega).

Clonogenic Assay

A monolayer of cancer cells was treated with 10 μM CRLX101 (CPT equivalents), 10 μM CPT, or PBS (control) for 24 hours, washed with fresh media, and then irradiated at 0, 1, 2, 4, or 6 Gy. After treatment, cells were plated into 25mL flasks at densities ranging from 100 to 250,000/plate. Cells were incubated for 13 days, fixed, and then stained with 4% formaldehyde /80% methanol /0.25% crystal violet (Fisher Scientific). All colonies containing 30 or more cells were counted. Plating efficiency (PE) was determined for each cell line. Surviving fraction (SF) was calculated using the formula [# of colonies/(# of plated cells)(PE)]. SF was plotted against radiation dose on a log scale. The linear-quadratic formula [$SF = e^{-\alpha D - \beta D^2}$] was used to generate survival curves using R package "CFAssay".

In Vitro Histone H2AX Phosphorylation and HIF-1 α Inhibition

HT-29 cells were irradiated with 2 Gy, washed with PBS, and then treated with 10 μM CPT, CRLX101, or PBS (control) diluted in culture medium. After 1, 12, or 48 h, the cells were processed for either immunofluorescence or western blot analysis.

Western Blot

Cells were lysed in RIPA lysis buffer (25mM Tris-HCl (pH 7.6), 150mM NaCl, 1% NP-40, 1% sodium deoxycholate, 0.1% SDS) supplemented with a protease and phosphatase inhibitor cocktail (Thermo Scientific) at the indicated times post irradiation. Protein concentration was determined using bicinchoninic acid protein assay (Pierce). The primary antibodies used were anti-Human HIF-1α (Novus Biologicals, Cat #NB100-479), VEGF (A-20) (Santa Cruz Biotechnology, Cat #sc152), and β-Actin (Cell Signaling, Cat #4970). The secondary antibodies used were anti-Rabbit or anti-Mouse IgG HRP-linked antibodies (Cell Signaling). The intensity of protein bands on the western blot image was quantified using Image J software. Ratios of HIF-1α and VEGF protein levels after β-Actin normalization were calculated from three independent experiments.

Immunofluorescence

Cells were fixed in 4% formaldehyde for 30 min, rinsed with PBS, and incubated in goat blocking solution (2% goat serum, 1% BSA, 0.1% Triton X-100, and 0.05% Tween 20) or

5% BSA blocking solution for 1 hour. After blocking, cells were stained with anti-Human HIF-1α (BD Transduction Laboratories, Cat #610958) or anti-Phospho-Histone H2AX (Ser139) antibodies (Millipore, Cat #05-636) for 1 hour at room temperature. Cells were then washed with PBS and further incubated with secondary antibody Alexa Fluor 568 Goat anti-Mouse IgG antibody (Molecular Probes, Cat #A11004) or Alexa Fluor 594 Donkey anti-Mouse IgG antibodies (Molecular Probes, Cat #A21203) for 30 min. After washing, cells were mounted using ProLong Gold Antifade Mountant with DAPI (Molecular Probes, Cat #P36935). HIF-1α immunofluorescent images were acquired using an Olympus BX61 fluorescence microscope (40× objective lens). γH2AX immunofluorescent images were acquired using a Zeiss LSM 700 laser scanning confocal microscope with z-stack sectioning (63× oil immersion objective lens). To minimize the overlap of foci, images were stacked by maximum intensity projection. The number of γH2AX foci per cell was counted using Image J software.

Immunohistochemistry of Tissue Sections

For immunohistochemical studies of tumor xenografts, HT-29 cells (1×10^6 cells in 200 μL in 1:1 DMEM/F12 and Matrigel) were inoculated subcutaneously into the left dorsal flanks of 8-week-old male Nu/Nu mice. Eleven days after inoculation, mice were treated with CRLX101 (5 mg/kg), CPT (5 mg/kg) or PBS (control) and given a single 5 Gy dose of radiation 1 hour later. Mice were sacrificed at 1 and 7 days after radiation treatment, and tumor samples were harvested for histology. Tumors were fixed in 4% formaldehyde for 24–48 hours at 4°C, paraffin embedded, and cut into 6 μm sections. For GI toxicity assays, colons were flushed with PBS and fixed overnight in 4% PFA. Tissues were then transferred to 30% sucrose for 24 hours, cut longitudinally, "swiss rolled", and embedded in Optimal Cutting Temperature (OCT) compound. Using a cryotome, 8 μm sections of OCT embedded tissues were taken and placed onto microscope slides. Sections were immersed in blocking solution (2% goat serum, 1% BSA, 0.1% Triton X-100, and 0.05% Tween 20) for 1 hour. After blocking, sections were incubated with primary antibodies overnight at 4°C. Three primary antibodies were used: CAIX Antibody (H-120) (Santa Cruz, sc-25599), VEGF Antibody (A-20) (Santa Cruz, sc-152), and Cleaved Caspase-3 (Asp175) (Cell Signaling, 9661). The secondary antibodies used were Alexa Fluor 594 Goat anti-Rabbit IgG Antibody or Alexa Fluor 568 Goat anti-Mouse IgG Antibody (Molecular Probes). Slides were mounted using ProLong Gold Antifade Mountant with DAPI (Molecular Probes, Cat #P36935). Images were acquired using a Zeiss LSM 700 Confocal microscope.

GI Toxicity

C57BL/6J mice were intravenously injected with 1 dose of CRLX101 (5 mg/kg), CPT (5 mg/kg), or PBS (control) and given 3 fractions of radiation at 5 Gy daily (15 Gy total). Tissues were then collected, processed, and stained for Cleaved Caspase 3. Toxicity was evaluated at 2, 4, and 14 days after treatment by quantifying the number of Cleaved Caspase-3 positive cells per crypt unit. A minimum of 50 crypt units were quantified for each sample.

Hair Toxicity

C57BL/6J mice were intravenously injected with a single intravenous dose of CRLX101 5 mg/kg), CPT (5 mg/kg), or PBS (control) and sequentially subjected to a radiation dose of 15 Gy (1 fraction). After 49 days, mice were evaluated for hair loss.

In Vivo Drug Efficacy

Tumors were established by subcutaneous injection of cancer cells suspended in 200 uL 1:1 DMEM:F12 and Matrigel into the left dorsal flank of 6- to 8-week-old male Nu/Nu mice. For HT-29 tumor xenografts, 1×10^6 cells were injected. For SW480 tumor xenografts, 2.5 $\times 10^6$ cells were injected. Treatment began ten days after tumor inoculation, or when tumors reached 100 to 150 mm^3. Mice were weighed and randomly sorted into treatment groups (8–10 mice per group). To evaluate drug efficacy of CRLX101 as a radiosensitizer *in vivo*, a single dose of CRLX101 (5 mg/kg) with or without 5-FU (20 mg/kg) was administered by tail-vein intravenous (I.V.) injection. To evaluate CRLX101 plus 5-FU combined chemoradiotherapy with other combination regimens, CRLX101 (5 mg/kg), oxaliplatin (16.7 mg/kg, equivalent to 50 mg/m^2 in human), and/or 5-FU (20 mg/kg) were administered to tumor bearing mice via tail-vein I.V. injection. Mice were irradiated with three fractions of radiation at 5 Gy (15 Gy total) daily. The first fraction of radiation was administered one hour after injection. Tumor volumes were determined by measuring two perpendicular diameters, *a* and *b*, using the formula [$V = 0.5 \times a \times b^2$] (*a* and *b* represent the long and short perpendicular diameters respectively). Measurements were recorded every 2 to 3 days using a digital caliper. The relative tumor size was defined by V/V_0, where V represents the tumor volume over time and V_0 represents the initial tumor volume. Mice were euthanized when the tumor volume reached 5 times the initial volume.

Cell Repopulation Assay

HT-29 cells were treated with CRLX101 (37.5 ng/mL), 5-FU (0.15 μg/mL), CRLX101 + 5-FU (37.5 ng/mL and 0.15 μg/mL, respectively), or PBS (control) for 48 hours and irradiated with 4 Gy. After treatment, 1×10^5 treated HT-29 cells were mixed and seeded with 1000 untreated HT-29-luc2 cells in 6 well plates. Luciferase activity was recorded every 2 to 3 days over 13 days using IVIS Kinetic Optical System (Caliper Life Sciences). Images were taken 10 min after adding D-luciferin substrate solution (System Biosciences).

Statistical Analysis

Results from histological analysis, western blot assays, and MTS assays were statistically assessed by either one-way or two-way ANOVA followed by Tukey's honestly significant difference post hoc test (if a positive F test was detected). For clonogenic assays, linear-quadratic cell survival curves were analyzed using R package "CFAssay". For tumor growth curve and luciferase activity experiments, we used area under the growth curve (AUC). The Wilcoxon rank sum test was used to compare the growth rates as previously described (32). P-values less than 0.05 were considered significant.

Results

CRLX101 is a potent radiosensitizer in vitro

CRLX101 was evaluated as a radiosensitizer *in vitro* using two colorectal cancer cell lines: HT-29 and SW480. To determine the direct cytotoxic impact of CRLX101 on each cell line, we generated dose-response curves in the absence of radiation (Figure 1A). We found that the direct cytotoxicity of CRLX101 was generally lower than the cytotoxicity of CPT. The IC_{50} values of CRLX101 were higher for both HT-29 and SW480 cells. Additionally, SW480 cells treated with CRLX101 demonstrated higher rates of survival across all treatment concentrations when compared to cells treated with CPT (Figure 1A). We then compared the radiosensitizing effects of CRLX101 and CPT using radiation survival curves. We found that CRLX101 and CPT both act as potent radiosensitizers in HT-29 and SW480 cells (Figure 1B). Sensitization enhancement ratios (SER) were calculated as the ratio of doses required to achieve 10% surviving fraction of cells. The SERs for CPT were 2.2 for HT-29 and 1.5 for SW480. At equivalent drug concentrations, the SERs for CRLX101 were 2.3 for HT-29 and 1.3 for SW480.

CRLX101 inhibits DNA damage repair

The induction of DNA double strand breaks (DSBs) by ionizing radiation or cytotoxic agents causes histone variant H2AX to become rapidly phosphorylated at serine 139 (γH2AX) and to form discrete nuclear foci. To examine if CRLX101 inhibits DNA repair following radiation damage, γH2AX foci formation and persistence was analyzed using immunofluorescence. At 1 hour following radiation damage, we observed equivalent γH2AX foci formation in all treatment conditions (Figure 2A). At 12 hours following radiation damage, we observed a significant decrease in the number of γH2AX foci in untreated control cells, suggesting successful DNA repair. In contrast, we observed an increase in the number of γH2AX foci in cells treated with either CRLX101 or CPT ($p<0.001$) (Figure 2B). These results indicate that CRLX101 and CPT promote radiosensitization by directly inducing additional DNA damage and/or inhibiting DNA repair.

CRLX101 inhibits radiation induced HIF-1α activation in vitro and in vivo

Cancer cells evade radiation-induced apoptosis in part through activation of HIF-1α signaling (33,34). To examine the effect that CRLX101 has on HIF-1α signaling after radiation damage, we assessed HIF-1α expression levels in HT-29 cells following radiotherapy. At 1 hour following radiation damage, control cells and cells treated with either CRLX101 or CPT all demonstrated similar HIF-1α expression levels (Figure 3A and 3B). At 12 hours following radiation damage, however, the expression of HIF-1α was significantly lower in cells treated with either CPT or CRLX101 when compared to levels of HIF-1α present in control cells (Figure 3A). We found that the expression of HIF-1α was suppressed by CRLX101 for at least 48 hours, as shown by western blot analysis (Figure 3B).

HIF-1α directly up-regulates the expression of genes that are involved in tumor angiogenesis (e.g. VEGF), pH balance (e.g. CAIX), and glucose metabolism (25,35). To determine the

effect of CRLX101 on downstream HIF-1α signaling, we assessed the expression of VEGF and CAIX in tumors using immunofluorescence. Mice bearing HT-29 xenograft tumors were treated with CRLX101, CPT, or PBS (control) and then irradiated. One day following treatment, we observed similar levels of VEGF expression in tumors from control animals and animals treated with either CPT or CRLX101 (Figure 3C). Seven days following treatment, however, we found that tumors from mice treated with either CPT or CRLX101 showed significantly less VEGF expression when compared to tumors taken from control animals (Figure 3D). In addition to VEGF expression, we also assessed the expression of CAIX. We found that tumors from control animals and animals treated with CPT demonstrated prominent CAIX expression at 1 and 7 days after treatment. In contrast, we found that tumors from animals treated with CRLX101 demonstrated a modest reduction of CAIX expression at 1 day post-treatment followed by a more prominent reduction of CAIX expression at 7 days post-treatment (Figure 3C and 3D).

CRLX101 is a potent radiosensitizer and improves 5-FU-based rectal cancer chemoradiotherapy in xenograft models

We next sought to evaluate the efficacy of CRLX101 as a radiosensitizer *in vivo*. Given that 5-FU is part of the standard CRT regimen for rectal cancer, we assessed the therapeutic efficacies of combining radiotherapy with CRLX101, 5-FU, or CRLX101 and 5-FU using murine rectal cancer xenograft models. We chose a flank xenograft model over an orthotopic model for the ease of measuring tumor volume over time. Immunodeficient mice bearing either HT-29 or SW480 xenografts were treated with a single dose of chemotherapy followed by three daily fractions of radiotherapy (5 Gy × 3). In SW480 xenografts, radiotherapy combined with CRLX101 delayed tumor growth more than radiotherapy combined with 5-FU (CRLX101+XRT vs. 5-FU+XRT: p-value = 0.0006) (Figure 4B). In mice bearing HT-29 tumor xenografts, the greatest therapeutic efficacy was observed when CRLX101 and 5-FU were combined with radiotherapy (5-FU+CRLX101+XRT vs. CRLX101+XRT: p-value = 0.001) (Figure 4A). Our results show that the addition of CRLX101 to 5-FU-based CRT significantly improves the therapeutic index.

While oxaliplatin (Ox) has been studied extensively in rectal cancer CRT, clinical studies suggest that it does not enhance the therapeutic index of standard CRT regimens. To determine whether CRLX101 enhances standard rectal cancer CRT more than Ox, we assessed the therapeutic efficacies of combining radiotherapy with 5-FU, 5-FU and Ox, and 5-FU and CRLX101 using HT-29 and SW480 murine xenograft models. As shown in Figure 4C and 4D, the slowest tumor growth was observed in animals treated with radiotherapy and both 5-FU and CRLX101. Consistent with clinical studies, the addition of Ox to 5-FU CRT did not improve the therapeutic efficacy of standard CRT. These data suggest that CRLX101 acts synergistically with 5-FU to suppress tumor growth.

5-FU can inhibit tumor repopulation after CRLX101-based CRT

To determine why the combination of CRLX101 and 5-FU CRT had the highest therapeutic efficacy *in vivo*, we examined the effect of different CRT regimens on repopulation rates of untreated HT-29 cells *in vitro* using a previously established repopulation assay (36). Briefly, we mixed a small number of untreated, luciferase-labeled HT-29 (HT-29-luc2) cells

with a larger number of treated, unlabeled HT-29 cells and assessed the growth rate of untreated HT-29-luc2 cells via luciferase activity over time (Figure 5A). Note that there is a strong linear correlation between bioluminescence and HT-29-luc2 cell numbers (R^2=0.9953) (Supplementary Figure S1). When compared to cells treated with PBS or 5-FU plus radiation, cells treated with CRLX101 and radiation or the combination of CRLX101, 5-FU, and radiation significantly increased the proliferation rate of co-cultured untreated HT-29-luc2 cells (Figure 5B). These results indicate that cells treated with CRLX101 or CRLX101 and 5-FU promote accelerated repopulation. Importantly, untreated HT-29-luc2 cells co-cultured with cells treated with 5-FU and CRLX101 demonstrated a lower proliferation rate when compared to cells co-cultured with cells treated with CRLX101 alone (p-value = 0.049) (Figure 5B and 5C). These results suggest that by limiting accelerated cell repopulation, the combination of CRLX101, 5-FU, and radiation has a greater therapeutic efficacy than CRLX101 plus radiation *in vivo*.

CRLX101 has low in vivo toxicity

We evaluated the toxicity profile of CRLX101-based CRT by investigating hair toxicity of CRLX101-based CRT in mice. We compared the toxicity profile of combining radiotherapy with CRLX101, CPT or PBS (control). At 49 days post irradiation, we observed hair change in 75% of CRLX101 treated animals, 100% of CPT treated animals, and 57% of animals receiving PBS (Supplementary Figure S2). Mice treated with either CRLX101 or PBS and radiotherapy exhibited no alopecia. In contrast, we observed alopecia in 43% of mice treated with CPT and radiotherapy (Supplementary Figure S2).

Gastrointestinal toxicity is one of the most commonly encountered and clinically relevant toxicities experienced during CRT in rectal cancer patients. To evaluate GI toxicity, we quantified the number of cells undergoing radiation induced apoptosis in the colonic tissues of animals receiving PBS, CPT, or CRLX101 and fractionated radiation (5Gy $\times$ 3) by immunostaining for Cleaved Caspase 3, a marker of apoptosis. We found that animals treated with radiotherapy and CPT or CRLX101 demonstrated higher GI toxicities than animals treated with radiation only. Importantly, the GI toxicity observed in animals treated with radiotherapy and CRLX101 was significantly lower than animals treated with radiotherapy and CPT (Figure 6A). Notably, animals in all treatment arms demonstrated normal colonic morphology at 14 days post treatment (Figure 6B).

Discussion

The recent development of CRLX101, a nanoparticle-drug conjugate containing CPT as the payload, offers a unique opportunity to revisit the use of topo-1 inhibitors in CRT for rectal cancer treatment. This development may facilitate the clinical translation of CPT into CRT regimens for rectal cancer. Clinical trials have demonstrated that CRLX101 has a favorable toxicity profile and its dual function (inhibition of both topo-1 and HIF-1α) makes it a promising radiosensitizer for use in CRT.

Although CPT is known to be a potent radiosensitizer (37), incorporation of CPT into a nanoparticle formulation may affect its radiosensitizing efficacy. Hence, we first examined the potency of CRLX101 as a radiosensitizer *in vitro*. We found that CRLX101 is as

effective as free CPT at radiosensitizing rectal cancer cells *in vitro*. We did not find CRLX101 to be superior to CPT in *in vitro* radiosensitization, since the EPR effect is an *in vivo* phenomenon. Inhibition of post-radiation DNA repair is one mechanism responsible for radiosensitization. CPT is known to promote radiosensitization by inhibiting topo-1 and directly causing DNA damage while preventing successful DNA repair. Consistent with this mechanism, we found that CRLX101 promotes radiosensitization in part by promoting the formation and persistence of radiation induced DSBs. Another mechanism for promoting radiosensitization is by inhibiting pro-survival pathways. Given that radiotherapy is known to induce HIF-1α signaling, a pathway that promotes radio-resistance in cancer cells (25,38), we examined the effect of CRLX101 on HIF-1α activity following radiation damage. Consistent with previous studies investigating the effects of combining CRLX101 with bevacizumab, our data showed that CRLX101 inhibits HIF-1α up-regulation in a prolonged manner (38). Importantly, HIF-1α inhibition resulted in reduced expression of downstream HIF-1α signaling targets, including CAIX and VEGF (25). Although both CPT and CRLX101 inhibit radiation induced HIF-1α expression, CRLX101 led to a more sustained inhibition of HIF-1α expression, likely due to prolonged CPT release.

Since HIF-1α has been implicated in promoting resistance to radiotherapy (34), the ability of CRLX101 to inhibit HIF-1α in addition to topo-1 has the potential of increasing the efficacy of rectal cancer CRT. We validated our *in vitro* findings using a subcutaneous mouse xenograft model of rectal cancer, a model that has been widely used in preclinical studies. We demonstrated that CRLX101 is indeed a potent radiosensitizer *in vivo*. We also found that in HT-29 and SW480 xenografts, the administration of a CRT regimen containing both 5-FU and CRLX101 had the highest therapeutic efficacy. This finding suggests that the optimal CRT regimen for rectal cancer treatment should include both CRLX101 and 5-FU. We hypothesized that 5-FU enhanced the efficacy of CRLX101-based CRT by preventing accelerated repopulation inhibition. Accelerated repopulation following radiotherapy is a well-known phenomenon that contributes to the local recurrence of tumors (39). During accelerated repopulation, growth-stimulating signals from dying cells promote rapid proliferation of surviving tumor cells after treatment (36,40). To examine this possibility, we utilized an established repopulation assay and found that while CRLX101-based CRT treatment promoted accelerated repopulation, the addition of 5-FU to CRLX101-based CRT negated this effect. These data suggest that 5-FU acts synergistically with CRLX101 *in vivo* to suppress tumor growth after CRT by inhibiting accelerated repopulation. Taken together, these preclinical findings support the clinical use of CRT treatment regimens that contain both 5-FU and CRLX101.

Although promising in preclinical studies, clinical trials investigating the use of Ox in rectal cancer CRT have not shown sufficient enhancement of CRT efficacy to support its use. Consistent with previous data, the addition of Ox to 5-FU-based CRT did not improve therapeutic efficacy in our mouse xenograft model of rectal cancer. Importantly, we found that combining radiotherapy with CRLX101 and 5-FU is significantly more effective than combining radiotherapy with Ox and 5-FU. These *in vivo* results provide strong evidence to support clinical testing of CRLX101 as an additive to standard rectal cancer CRT. While these results are encouraging, it is important to point out that other factors, such as chemotherapeutic bioavailability, may have influenced the outcome of this preclinical study.

Lastly, we also examined the potential toxicity of CRLX101-based CRT to normal tissues *in vivo*. Radiation elevates vascular permeability within both tumor and normal tissues (41–43). We assessed the effect that adding CRLX101 to radiotherapy had on GI toxicity by examining apoptosis rates in colonic tissues shortly following radiation damage. We found that the addition of CRLX101 to radiotherapy resulted in lower rates of radiation-induced apoptosis when compared to animals treated with CPT and radiotherapy. There was, however, some evidence of GI toxicity in animals treated with CRLX101 and radiotherapy, possibly due to increased vascular permeability following radiation damage. In addition to evaluating GI toxicity, we also evaluated mouse hair toxicity as a surrogate for skin and mucosal surface toxicity. We demonstrated that while the addition of CRLX101 did increase hair toxicity, the effect is mild. We hypothesize that this finding will not be clinically significant.

In summary, these preclinical data demonstrate that CRLX101 is a potent radiosensitizer with the potential of improving rectal cancer CRT. CRLX101 functions by inhibiting both topo-1 and the HIF-1α signaling. Our data indicate that CRLX101 and 5-FU may be an optimal CRT regimen for rectal cancer treatment. Our preclinical data support the ongoing Phase Ib/II clinical trial, LCCC1315, titled "Neoadjuvant Chemoradiotherapy with CRLX-101 and Capecitabine for Rectal Cancer" (ClinicalTrials.gov Identifier: NCT02010567).

Supplementary Material

Refer to Web version on PubMed Central for supplementary material.

Acknowledgments

References

1. Siegel R, DeSantis C, Virgo K, Stein K, Mariotto A, Smith T, et al. Cancer treatment and survivorship statistics, 2012. CA Cancer J Clin. 2012; 62:220–241. [PubMed: 22700443]

2. Minsky BD, Cohen AM, Kemeny N, Enker WE, Kelsen DP, Reichman B, et al. Combined modality therapy of rectal cancer: decreased acute toxicity with the preoperative approach. J Clin Oncol. 1992; 10:1218–1224. [PubMed: 1634912]

3. Sauer R, Liersch T, Merkel S, Fietkau R, Hohenberger W, Hess C, et al. Preoperative versus postoperative chemoradiotherapy for locally advanced rectal cancer: results of the German CAO/ARO/AIO-94 randomized phase III trial after a median follow-up of 11 years. J Clin Oncol. 2012; 30:1926–1933. [PubMed: 22529255]

4. Tepper JE, O'Connell MJ, Petroni GR, Hollis D, Cooke E, Benson AB 3rd, et al. Adjuvant postoperative fluorouracil-modulated chemotherapy combined with pelvic radiation therapy for rectal cancer: initial results of intergroup 0114. J Clin Oncol. 1997; 15:2030–2039. [PubMed: 9164215]

5. Krook JE, Moertel CG, Gunderson LL, Wieand HS, Collins RT, Beart RW, et al. Effective surgical adjuvant therapy for high-risk rectal carcinoma. N Engl J Med. 1991; 324:709–715. [PubMed: 1997835]

6. Fisher B, Wolmark N, Rockette H, Redmond C, Deutsch M, Wickerham DL, et al. Postoperative adjuvant chemotherapy or radiation therapy for rectal cancer: results from NSABP protocol R-01. J Natl Cancer Inst. 1988; 80:21–29. [PubMed: 3276900]

7. Sauer R, Becker H, Hohenberger W, Rodel C, Wittekind C, Fietkau R, et al. Preoperative versus postoperative chemoradiotherapy for rectal cancer. N Engl J Med. 2004; 351:1731–1740. [PubMed: 15496622]

8. Willett CG, Duda DG, Ancukiewicz M, Shah M, Czito BG, Bentley R, et al. A safety and survival analysis of neoadjuvant bevacizumab with standard chemoradiation in a phase I/II study compared with standard chemoradiation in locally advanced rectal cancer. Oncologist. 2010; 15:845–851. [PubMed: 20667969]

9. Willett CG, Duda DG, di Tomaso E, Boucher Y, Ancukiewicz M, Sahani DV, et al. Efficacy, safety, and biomarkers of neoadjuvant bevacizumab, radiation therapy, and fluorouracil in rectal cancer: a multidisciplinary phase II study. J Clin Oncol. 2009; 27:3020–3026. [PubMed: 19470921]

10. Crane CH, Eng C, Feig BW, Das P, Skibber JM, Chang GJ, et al. Phase II trial of neoadjuvant bevacizumab, capecitabine, and radiotherapy for locally advanced rectal cancer. Int J Radiat Oncol Biol Phys. 2010; 76:824–830. [PubMed: 19464823]

11. Wong SJ, Winter K, Meropol NJ, Anne PR, Kachnic L, Rashid A, et al. Radiation Therapy Oncology Group 0247: a randomized Phase II study of neoadjuvant capecitabine and irinotecan or capecitabine and oxaliplatin with concurrent radiotherapy for patients with locally advanced rectal cancer. Int J Radiat Oncol Biol Phys. 2012; 82:1367–1375. [PubMed: 21775070]

12. Aschele C, Cionini L, Lonardi S, Pinto C, Cordio S, Rosati G, et al. Primary tumor response to preoperative chemoradiation with or without oxaliplatin in locally advanced rectal cancer: pathologic results of the STAR-01 randomized phase III trial. J Clin Oncol. 2011; 29:2773–2780. [PubMed: 21606427]

13. Ryan DP, Niedzwiecki D, Hollis D, Mediema BE, Wadler S, Tepper JE, et al. Phase I/II study of preoperative oxaliplatin, fluorouracil, and external-beam radiation therapy in patients with locally advanced rectal cancer: Cancer and Leukemia Group B 89901. J Clin Oncol. 2006; 24:2557–2562. [PubMed: 16636336]

14. de Campos-Lobato LF, Stocchi L, da Luz Moreira A, Geisler D, Dietz DW, Lavery IC, et al. Pathologic complete response after neoadjuvant treatment for rectal cancer decreases distant recurrence and could eradicate local recurrence. Ann Surg Oncol. 2011; 18:1590–1598. [PubMed: 21207164]

15. Park IJ, You YN, Agarwal A, Skibber JM, Rodriguez-Bigas MA, Eng C, et al. Neoadjuvant treatment response as an early response indicator for patients with rectal cancer. J Clin Oncol. 2012; 30:1770–1776. [PubMed: 22493423]

16. Young C, Schluep T, Hwang J, Eliasof S. CRLX101 (formerly IT-101)-A Novel Nanopharmaceutical of Camptothecin in Clinical Development. Curr Bioact Compd. 2011; 7:8–14. [PubMed: 22081768]

17. Habr-Gama A, Perez RO, Sao Juliao GP, Proscurshim I, Gama-Rodrigues J. Nonoperative approaches to rectal cancer: a critical evaluation. Semin Radiat Oncol. 2011; 21:234–239. [PubMed: 21645869]

18. Tepper JE, Wang AZ. Improving local control in rectal cancer: radiation sensitizers or radiation dose? J Clin Oncol. 2010; 28:1623–1624. [PubMed: 20194836]

19. Rodel C, Liersch T, Becker H, Fietkau R, Hohenberger W, Hothorn T, et al. Preoperative chemoradiotherapy and postoperative chemotherapy with fluorouracil and oxaliplatin versus fluorouracil alone in locally advanced rectal cancer: initial results of the German CAO/ARO/AIO-04 randomised phase 3 trial. Lancet Oncol. 2012; 13:679–687. [PubMed: 22627104]

20. Mehta VK, Cho C, Ford JM, Jambalos C, Poen J, Koong A, et al. Phase II trial of preoperative 3D conformal radiotherapy, protracted venous infusion 5-fluorouracil, and weekly CPT-11, followed by surgery for ultrasound-staged T3 rectal cancer. Int J Radiat Oncol Biol Phys. 2003; 55:132–137. [PubMed: 12504045]

21. Klautke G, Feyerherd P, Ludwig K, Prall F, Foitzik T, Fietkau R. Intensified concurrent chemoradiotherapy with 5-fluorouracil and irinotecan as neoadjuvant treatment in patients with locally advanced rectal cancer. Br J Cancer. 2005; 92:1215–1220. [PubMed: 15785742]

22. Glynne-Jones R, Falk S, Maughan TS, Meadows HM, Sebag-Montefiore D. A phase I/II study of irinotecan when added to 5-fluorouracil and leucovorin and pelvic radiation in locally advanced rectal cancer: a Colorectal Clinical Oncology Group Study. Br J Cancer. 2007; 96:551–558. [PubMed: 17262086]

23. Chen AY, Choy H, Rothenberg ML. DNA topoisomerase I-targeting drugs as radiation sensitizers. Oncology. 1999; 13:39–46. [PubMed: 10550825]

24. Eliasof S, Lazarus D, Peters CG, Case RI, Cole RO, Hwang J, et al. Correlating preclinical animal studies and human clinical trials of a multifunctional, polymeric nanoparticle. Proc Natl Acad Sci U S A. 2013; 110:15127–15132. [PubMed: 23980155]

25. Moeller BJ, Cao Y, Li CY, Dewhirst MW. Radiation activates HIF-1 to regulate vascular radiosensitivity in tumors: role of reoxygenation, free radicals, and stress granules. Cancer Cell. 2004; 5:429–441. [PubMed: 15144951]

26. Gaur S, Chen L, Yen T, Wang Y, Zhou B, Davis M, et al. Preclinical study of the cyclodextrin-polymer conjugate of camptothecin CRLX101 for the treatment of gastric cancer. Nanomedicine. 2012; 8:721–730. [PubMed: 22033079]

27. Weiss GJ, Chao J, Neidhart JD, Ramanathan RK, Bassett D, Neidhart JA, et al. First-in-human phase 1/2a trial of CRLX101, a cyclodextrin-containing polymer-camptothecin nanopharmaceutical in patients with advanced solid tumor malignancies. Invest New Drug. 2013; 31:986–1000.

28. Hobbs SK, Monsky WL, Yuan F, Roberts WG, Griffith L, Torchilin VP, et al. Regulation of transport pathways in tumor vessels: role of tumor type and microenvironment. Proc Natl Acad Sci U S A. 1998; 95:4607–4612. [PubMed: 9539785]

29. Jain RK, Stylianopoulos T. Delivering nanomedicine to solid tumors. Nat Rev Clin Oncol. 2010; 7:653–664. [PubMed: 20838415]

30. Svenson S, Wolfgang M, Hwang J, Ryan J, Eliasof S. Preclinical to clinical development of the novel camptothecin nanopharmaceutical CRLX101. J Control Release. 2011; 153:49–55. [PubMed: 21406204]

31. Schluep T, Cheng J, Khin KT, Davis ME. Pharmacokinetics and biodistribution of the camptothecin-polymer conjugate IT-101 in rats and tumor-bearing mice. Cancer Chemother Pharmacol. 2006; 57:654–662. [PubMed: 16133526]

32. Karve S, Werner ME, Sukumar R, Cummings ND, Copp JA, Wang EC, et al. Revival of the abandoned therapeutic wortmannin by nanoparticle drug delivery. Natl Acad Sci U S A. 2012; 109:8230–8235.

33. Semenza GL. Intratumoral hypoxia, radiation resistance, and HIF-1. Cancer Cell. 2004; 5:405–406. [PubMed: 15144945]

34. Harada H, Inoue M, Itasaka S, Hirota K, Morinibu A, Shinomiya K, et al. Cancer cells that survive radiation therapy acquire HIF-1 activity and translocate towards tumour blood vessels. Nature Commun. 2012; 3:783.

35. Potter C, Harris AL. Hypoxia inducible carbonic anhydrase IX, marker of tumour hypoxia, survival pathway and therapy target. Cell Cycle. 2004; 3:164–167. [PubMed: 14712082]

36. Donato AL, Huang Q, Liu X, Li F, Zimmerman MA, Li CY. Caspase 3 promotes surviving melanoma tumor cell growth after cytotoxic therapy. J Invest Dermatol. 2014; 134:1686–1692. [PubMed: 24434746]

37. Kim JH, Kim SH, Kolozsvary A, Khil MS. Potentiation of radiation response in human carcinoma cells in vitro and murine fibrosarcoma in vivo by topotecan, an inhibitor of DNA topoisomerase I. Int J Radiat Oncol Biol Phys. 1992; 22:515–518. [PubMed: 1310495]

38. Pham E, Birrer MJ, Eliasof S, Garmey EG, Lazarus D, Lee CR, et al. Translational impact of nanoparticle-drug conjugate CRLX101 with or without bevacizumab in advanced ovarian cancer. Clin Cancer Res. 2015; 21:808–818. [PubMed: 25524310]

39. Hittelman WN, Liao Y, Wang L, Milas L. Are cancer stem cells radioresistant? Future Oncol. 2010; 6:1563–1576. [PubMed: 21062156]

40. Huang Q, Li F, Liu X, Li W, Shi W, Liu FF, et al. Caspase 3-mediated stimulation of tumor cell repopulation during cancer radiotherapy. Nat Med. 2011; 17:860–866. [PubMed: 21725296]

41. Park HJ, Griffin RJ, Hui S, Levitt SH, Song CW. Radiation-induced vascular damage in tumors: implications of vascular damage in ablative hypofractionated radiotherapy (SBRT and SRS). Radiat Res. 2012; 177:311–327. [PubMed: 22229487]

42. Willoughby DA. Pharmacological aspects of the vascular permeability changes in the rat's intestine following abdominal radiation. Br J Radiol. 1960; 33:515–519. [PubMed: 13844999]

43. Park KR, Monsky WL, Lee CG, Song CH, Kim DH, Jain RK, et al. Mast Cells Contribute to Radiation-Induced Vascular Hyperpermeability. Radiat Res. 2016; 185:182–189. [PubMed: 26771172]
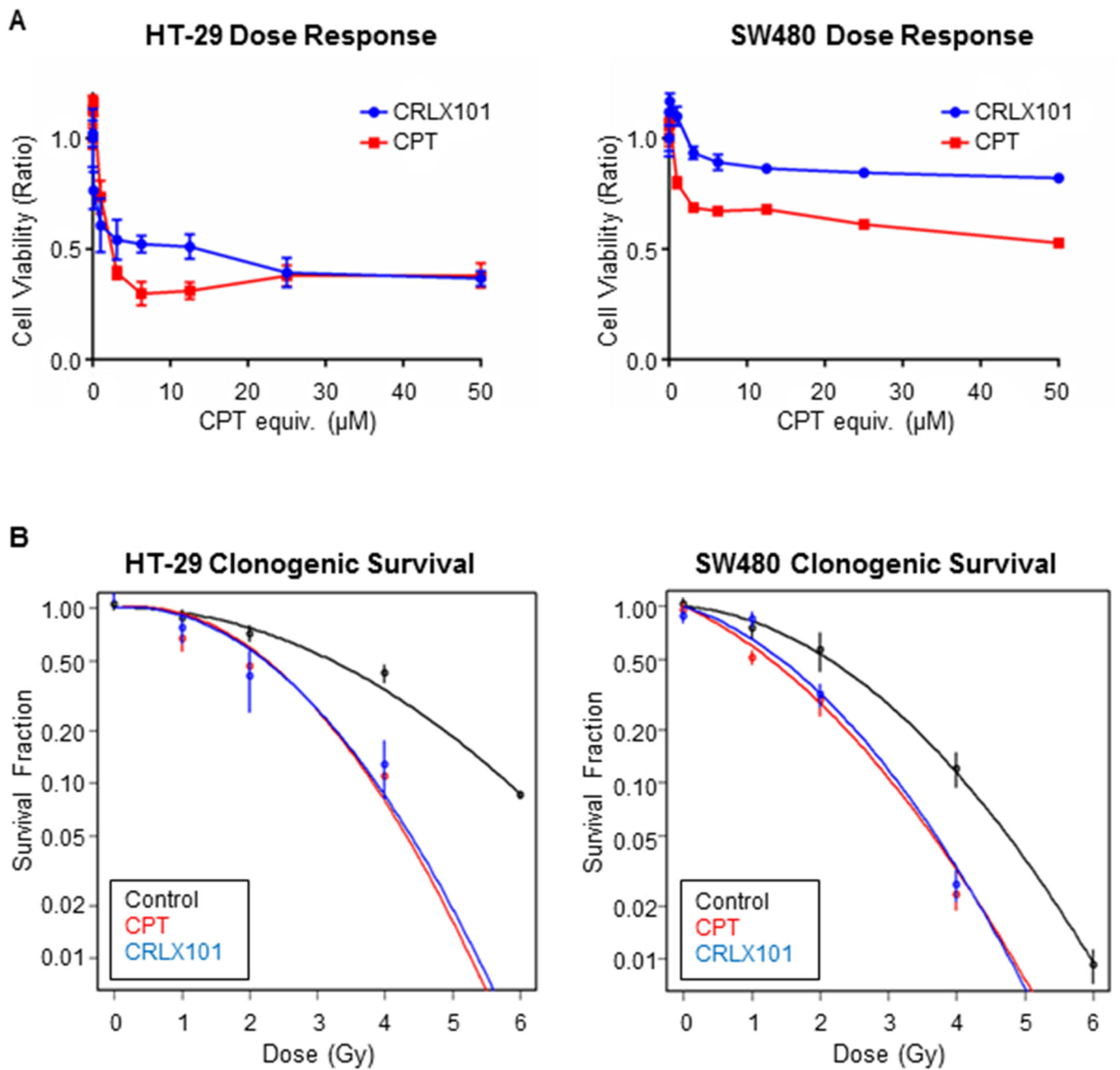
Figure 1.
Direct cytotoxicity and radiosensitization potential of CRLX101 treatment *in vitro*. (A) Cell viability of HT-29 and SW480 cells following 24 hours of CRLX101 or CPT treatment. (B) Clonogenic survival curves of HT-29 and SW480 cells treated with CRLX101 or CPT and radiation.
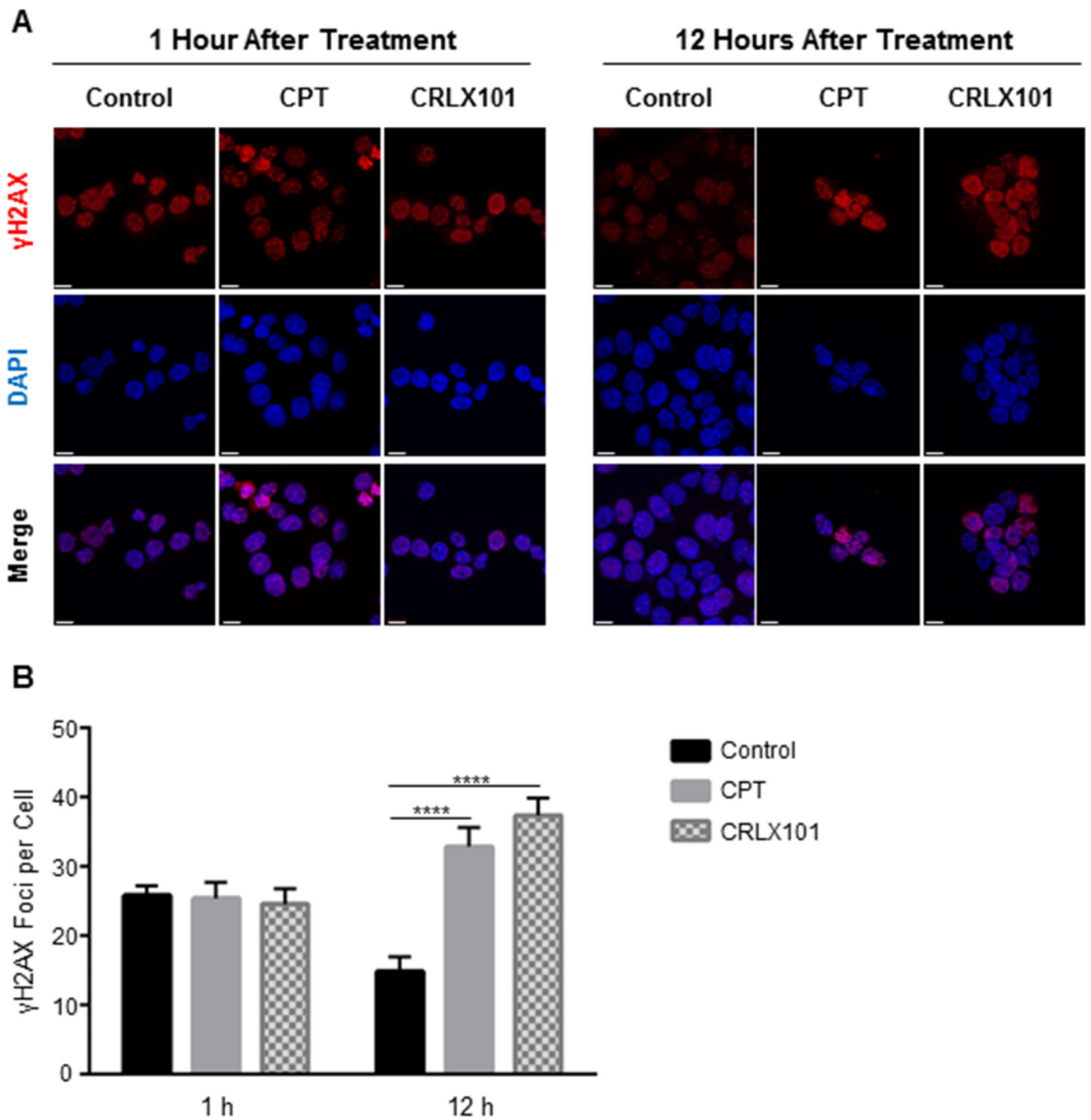
Figure 2.
Effect of CRLX101 treatment on radiation-induced DSB repair. (A) γH2AX foci formation (red) in nuclei (blue) of HT-29 cells following treatment with radiation and PBS (Control), CPT, or CRLX101. Scale bar = 10 μm. (B) Quantification of the number of γH2AX foci present in (A). ****p-value<0.001.
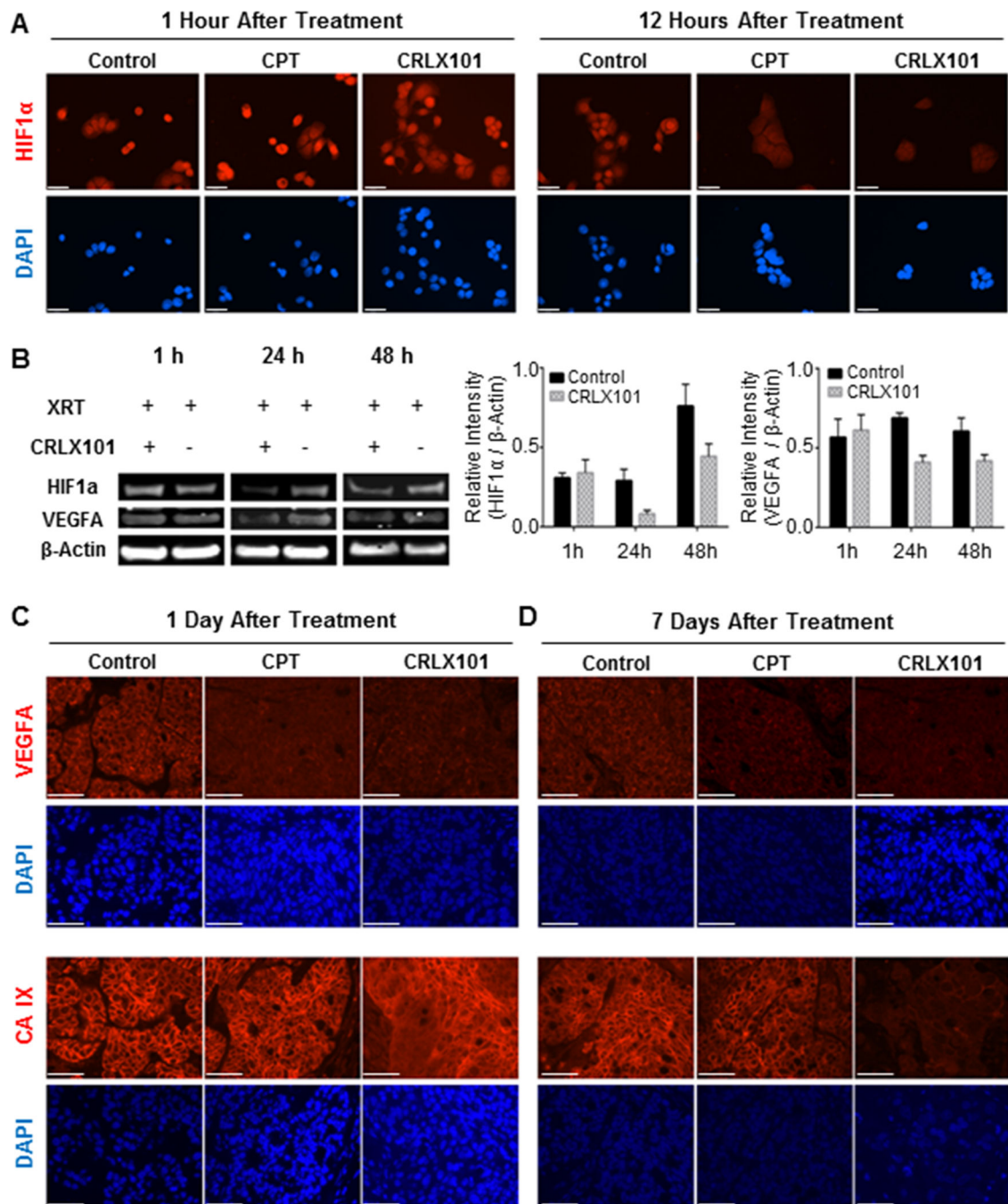
Figure 3.
Effect of CRLX101 on HIF-1α signaling following radiation. (A) Time course of HIF-1α expression (red) in the nuclei (blue) of HT-29 cells following treatment with radiotherapy and PBS (Control), CPT, or CRLX101. Scale bar = 16 μm. (B) Quantification of HIF-1α and VEGFA protein expression in HT-29 cells at various time points following treatment with radiation and PBS (Control) or CRLX101. (C-D). VEGFA and CAIX expression in xenograft tumors at 1 and 7 days after animals were treated with radiation and PBS (Control), CPT, or CRLX101. Scale bar = 50 μm.
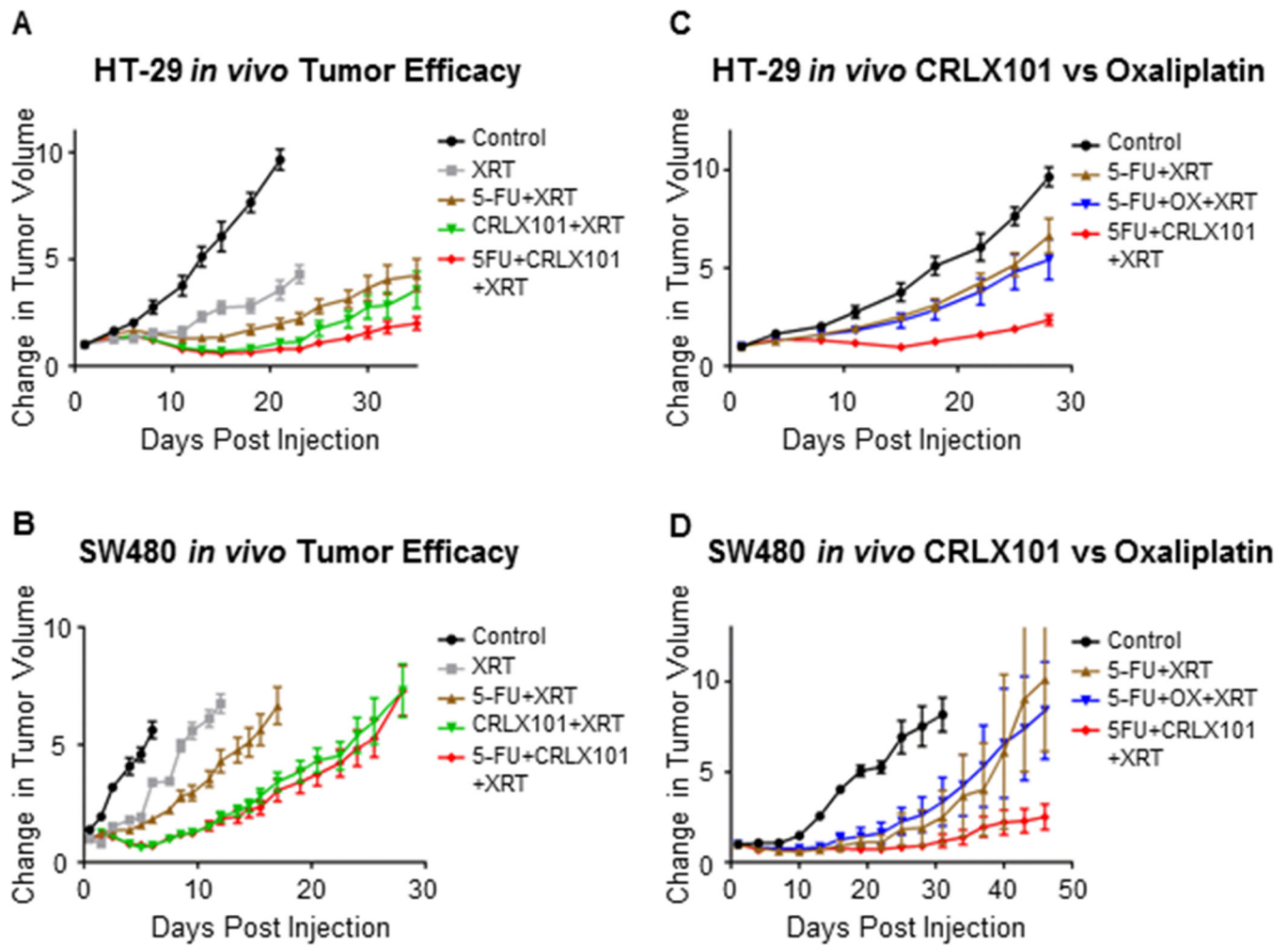
Figure 4.
Efficacy of CRLX101 CRT treatment on xenograft growth rates *in vivo*. Growth rates of HT-29 (A) and SW480 (B) tumor xenografts treated with radiation and 5-FU and/or CRLX101. Growth rates of HT-29 (C) and SW480 (D) tumor xenografts treated with 5-FU CRT and CRLX101 or Oxaliplatin (Ox).
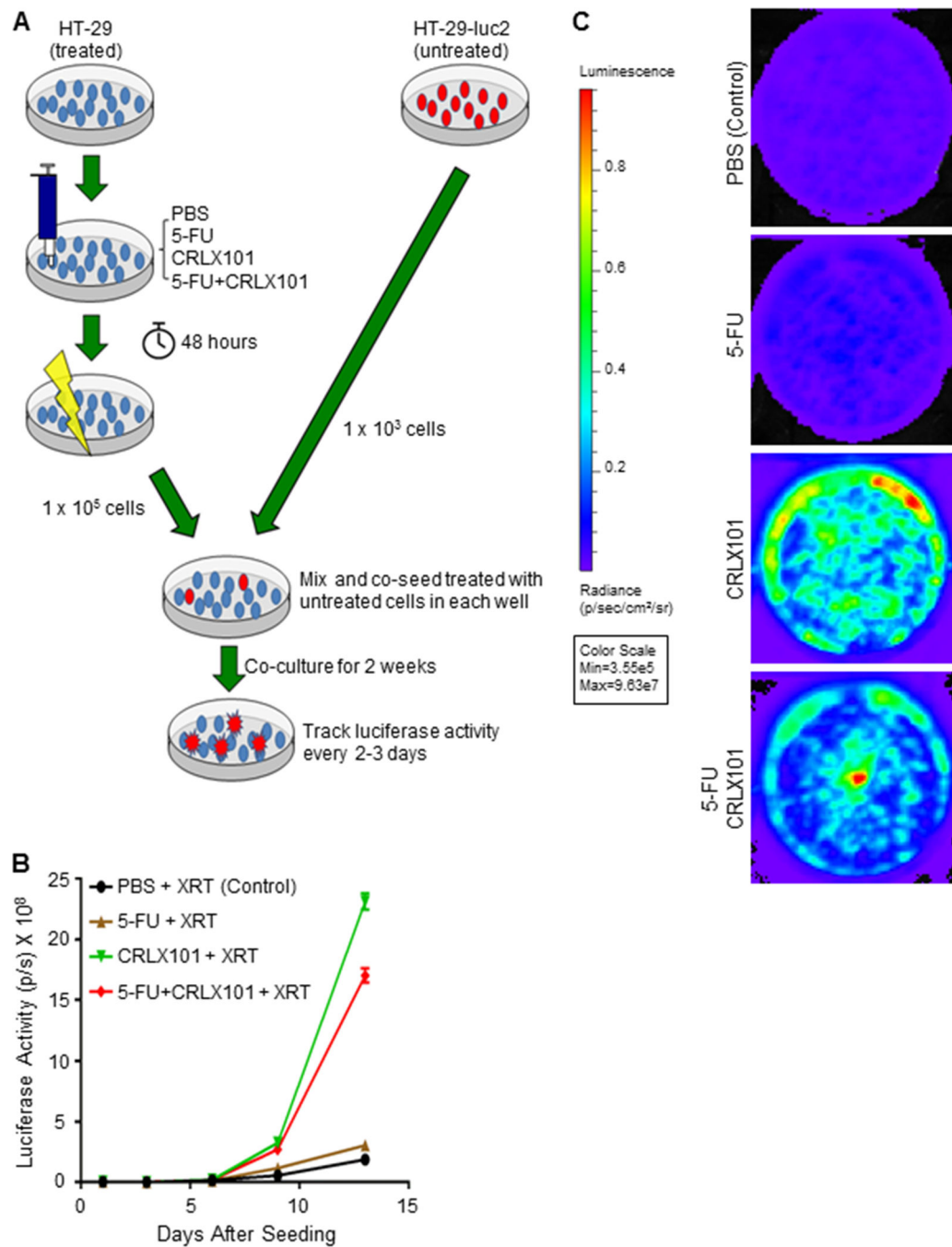
Figure 5.
Effect of CRLX101 on colorectal cancer cell repopulation. (A) Schematic drawing of *in vitro* cell repopulation assay. (B) Quantification of untreated HT-29-luc2 cell growth over time following treatment with radiation (XRT) and PBS (Control), 5-FU, CRLX101, or 5-FU and CRLX101. (C) Representative bioluminescence images of HT-29-luc2 cell cultures 13 days following treatment.
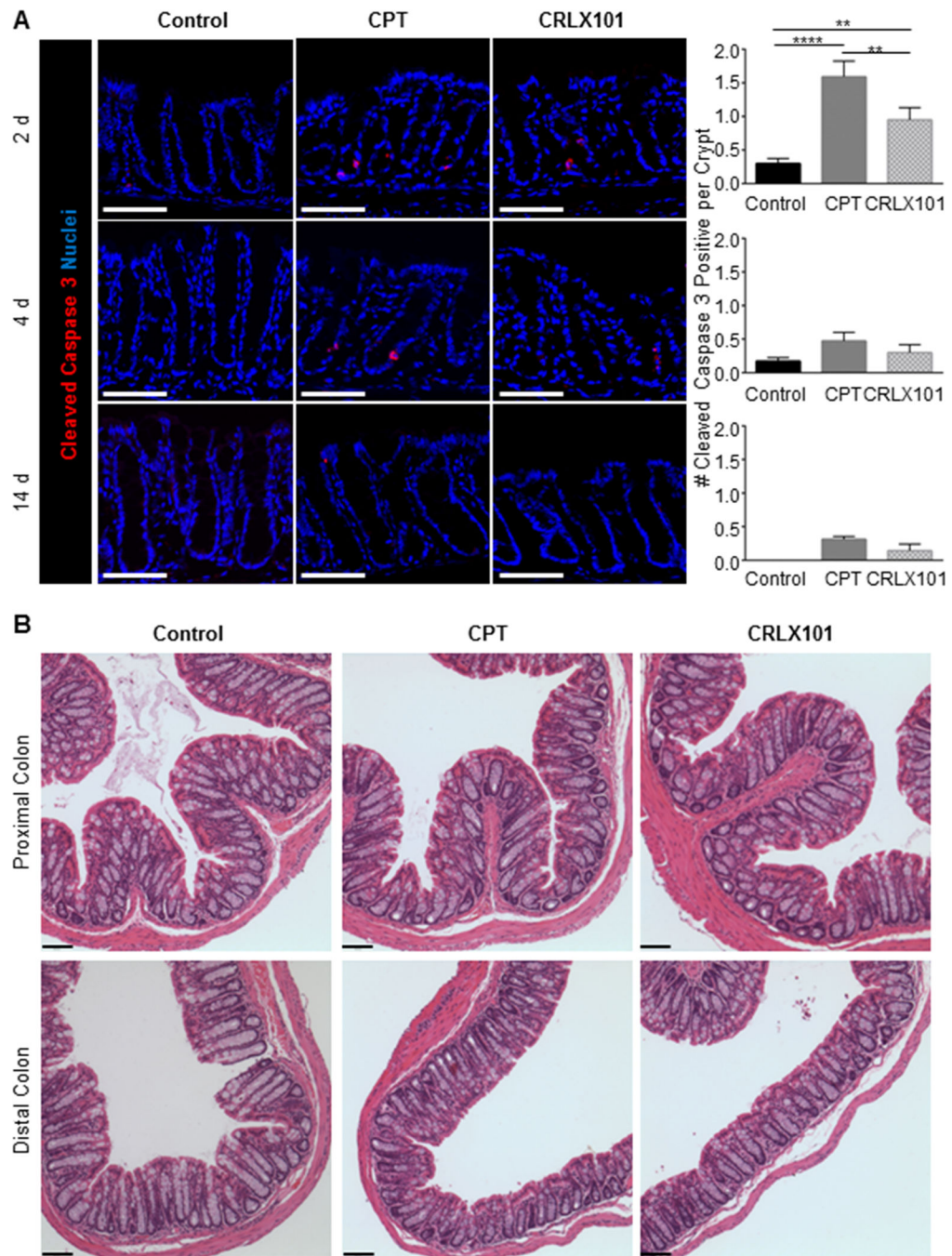
Figure 6.
Evaluation of GI toxicity following CRLX101 treatment. (A) Representative images and quantification of Cleaved Caspase 3 immunofluorescence in distal colon over time following treatment with PBS (Control), CPT, or CRLX101 and radiation. Scale bar = 50 μm. **P< 0.01, ****P <0.0001. (B) Representative images of H&E staining depicting global proximal and distal colonic morphology 14 days after treatment with PBS (Control), CPT, or CRLX101 and radiation. Scale bar = 80 μm.